PROCEEDINGS OF SCIENCE

Nucleon transverse momentum-dependent parton distributions from domain wall fermion calculations at 297 MeV pion mass

M. Engelhardt[*a†], **B. Musch**[b], **T. Bhattacharya**[c], **R. Gupta**[c], **P. Hägler**[b], **J. Negele**[d], **A. Pochinsky**[d], **A. Schäfer**[b], **S. Syritsyn**[e] **and B. Yoon**[c]

[a] *Department of Physics, New Mexico State University, Las Cruces, NM 88003, USA*
[b] *Institut für Theoretische Physik, Universität Regensburg, 93040 Regensburg, Germany*
[c] *Theoretical Division, Los Alamos National Laboratory, Los Alamos, NM 87545, USA*
[d] *Center for Theoretical Physics, Massachusetts Institute of Technology, Cambridge, MA 02139, USA*
[e] *RIKEN/BNL Research Center, Brookhaven National Laboratory, Upton, NY 11973, USA*
[†] *E-mail:* engel@nmsu.edu

Lattice QCD calculations of transverse momentum-dependent parton distributions (TMDs) in a nucleon are performed based on a definition of TMDs via hadronic matrix elements of quark bilocal operators containing staple-shaped gauge connections. A parametrization of the matrix elements in terms of invariant amplitudes serves to cast them in the Lorentz frame preferred for the lattice calculation. Using a RBC/UKQCD domain wall fermion ensemble corresponding to a pion mass of 297 MeV, on a lattice with spacing 0.084 fm, selected TMD observables are accessed and compared to previous explorations at heavier pion masses on coarser lattices.

The 32nd International Symposium on Lattice Field Theory
23-28 June, 2014
Columbia University, New York, NY

[*] Speaker.

PoS(LATTICE2014)167

1. Introduction

In the description of hadron structure, transverse momentum-dependent parton distribution functions [1] (TMDs) play a role complementary to generalized parton distributions (GPDs). Whereas GPDs encode information about the transverse spatial distribution of partons (through Fourier transformation with respect to the momentum transfer), TMDs contain information about the transverse momentum distribution of partons. Cast in a Lorentz frame in which the hadron of mass m_h propagates with a large momentum in the 3-direction, $P^+ \equiv (P^0 + P^3)/\sqrt{2} \gg m_h$, the quark momentum components scale such that TMDs are principally functions $f(x, k_T)$ of the quark longitudinal momentum fraction $x = k^+/P^+$ and the quark transverse momentum vector k_T, with the dependence on the component $k^- \equiv (k^0 - k^3)/\sqrt{2} \ll m_h$ becoming ignorable in this limit. The function $f(x, k_T)$ will thus be regarded as having been integrated over k^-.

Experimentally, TMDs manifest themselves in angular asymmetries observed in processes such as semi-inclusive deep inelastic scattering (SIDIS) and the Drell-Yan (DY) process. Corresponding signatures have emerged at COMPASS, HERMES and JLab [2–4], and that has motivated targeting a significant part of the physics program at future experiments in this direction, e.g., at the upgraded JLab 12 GeV facility and at the proposed electron-ion collider (EIC). Relating the experimental signature to the hadron structure encoded in TMDs requires a suitable factorization framework, the one having been advanced in [5–8] being particularly well-suited for connecting phenomenology to lattice QCD. Factorization in the TMD context is considerably more involved than standard collinear factorization, with the resulting TMDs in general being process-dependent, via initial and/or final state interactions between the struck quark and the hadron remnant.

2. Definition of TMD observables

The definition of TMD observables amenable to lattice evaluation has been laid out succinctly in a previous Lattice conference proceedings contribution [9], for a more detailed discussion, cf. [10]. Summarizing briefly, the starting point is the fundamental correlator

$$\widetilde{\Phi}^{[\Gamma]}_{\text{unsubtr.}}(b, P, S, \ldots) \equiv \frac{1}{2}\langle P,S|\ \bar{q}(0)\ \Gamma\ \mathscr{U}[0, \eta v, \eta v + b, b]\ q(b)\ |P,S\rangle \tag{2.1}$$

where S denotes the spin of the hadron and Γ stands for an arbitrary γ-matrix structure. The staple-shaped gauge connection $\mathscr{U}$ follows straight-line paths connecting the positions given in its argument; the unit vector v thus specifies the direction of the staple, whereas η parametrizes its length. The presence of $\mathscr{U}$ introduces divergences in $\widetilde{\Phi}^{[\Gamma]}_{\text{unsubtr.}}$ additional to the wave function renormalizations of the quark operators; these divergences accordingly must ultimately be compensated by additional "soft factors", which are expected to be multiplicative and do not need to be specified in detail here, since only appropriate ratios in which they then presumably cancel will ultimately be considered. In order to regularize rapidity divergences, the staple direction v is taken slightly off the light cone into the space-like region [5, 6], with perturbative evolution equations governing the approach to the light cone [7]. A useful parameter characterizing how close v is to the light cone is the Collins-Soper evolution parameter $\hat{\zeta} = v \cdot P/(|v|\,|P|)$, in terms of which the light cone is approached for $\hat{\zeta} \to \infty$. The correlator (2.1) can be decomposed in terms of invariant

amplitudes $\widetilde{A}_{iB}$. Listing only the components relevant for the Sivers and Boer-Mulders effects,

$$\frac{1}{2P^+}\widetilde{\Phi}^{[\gamma^+]}_{\text{unsubtr.}} = \widetilde{A}_{2B} + im_h\varepsilon_{ij}b_iS_j\widetilde{A}_{12B} \tag{2.2}$$

$$\frac{1}{2P^+}\widetilde{\Phi}^{[i\sigma^{i+}\gamma^5]}_{\text{unsubtr.}} = im_h\varepsilon_{ij}b_j\widetilde{A}_{4B} - S_i\widetilde{A}_{9B} - im_h\Lambda b_i\widetilde{A}_{10B} + m_h[(b\cdot P)\Lambda - m_h(b_T\cdot S_T)]b_i\widetilde{A}_{11B}\,, \tag{2.3}$$

where Λ denotes the hadron helicity (i.e., $S^+ = \Lambda P^+/m_h$, $S^- = -\Lambda m_h/2P^+$). These amplitudes are useful in that they can be evaluated in any desired Lorentz frame, including a frame which is particularly suited for the lattice calculation. Specializing to TMDs integrated over momentum fraction x, by considering specifically $b\cdot P = 0$, they serve to define the "generalized Sivers shift"

$$\langle k_y\rangle_{TU}(b_T^2,\ldots) = -m_h\widetilde{A}_{12B}(-b_T^2,\ldots)/\widetilde{A}_{2B}(-b_T^2,\ldots) = m_h\tilde{f}_{1T}^{\perp[1](1)}(b_T^2,\ldots)/\tilde{f}_1^{[1](0)}(b_T^2,\ldots) \tag{2.4}$$

where the right-hand expression introduces the notation in terms of Fourier-transformed TMD moments, for details, cf. [10]. In the $b_T \to 0$ limit, (2.4) formally represents the average transverse momentum k_y of unpolarized ("U") quarks orthogonal to the transverse ("T") spin of the hadron, normalized to the corresponding number of valence quarks. Analogously, one defines the "generalized Boer-Mulders shift"

$$\langle k_y\rangle_{UT}(b_T^2,\ldots) = m_h\widetilde{A}_{4B}(-b_T^2,\ldots)/\widetilde{A}_{2B}(-b_T^2,\ldots) = m_h\tilde{h}_1^{\perp[1](1)}(b_T^2,\ldots)/\tilde{f}_1^{[1](0)}(b_T^2,\ldots) \tag{2.5}$$

which in the $b_T \to 0$ limit formally represents the average transverse momentum k_y of quarks polarized in the transverse ("T") x-direction orthogonal to k_y, in an unpolarized ("U") hadron, again normalized to the corresponding number of valence quarks. The ratios (2.4) and (2.5) are designed to cancel both multiplicative soft factors associated with the gauge connection $\mathscr{U}$ as well as wave function renormalizations attached to the quark operators in (2.1) at finite physical separation b.

3. Lattice evaluation and results

To access generalized shifts such as (2.4) and (2.5) within lattice QCD, one calculates hadron matrix elements of the type (2.1) and then decomposes them into invariant amplitudes, as given in (2.2)-(2.3). For this to be possible, it is crucial to work in a scheme where the four-vectors b and v are generically space-like, for the following reason: By employing a Euclidean time coordinate to project out hadron ground states via Euclidean time evolution, lattice QCD cannot straightforwardly accomodate operators containing Minkowski time separations. The operator of which one takes matrix elements thus has to be defined at a single time. Only if both b and v are space-like is there no obstacle to boosting the problem to a Lorentz frame in which b and v are purely spatial, and evaluating $\widetilde{\Phi}^{[\Gamma]}_{\text{unsubtr.}}$ in that frame. The results extracted for the invariant amplitudes $\widetilde{A}_{iB}$ are then immediately valid also in the original frame in which (2.1) was initially defined, thus completing the determination of quantities of the type (2.4) and (2.5).

Since, in a numerical lattice calculation, the staple extent η necessarily remains finite, two extrapolations must be performed from the generated data, namely, the one to infinite staple length, $\eta \to \infty$, and the extrapolation of the staple direction towards the light cone, $\hat{\zeta} \to \infty$. Whereas the former extrapolation is under control for a range of parameters used in this work, the latter presents a challenge, owing to the limited set of hadron momenta P accessible with sufficient statistical

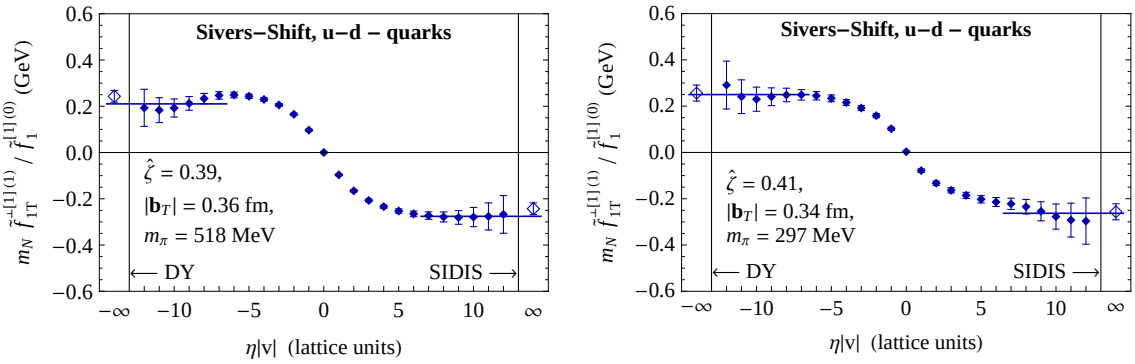

Figure 1: Dependence of the generalized Sivers shift on the staple extent at a fixed b_T and $\hat{\zeta}$, in a coarse lattice mixed action calculation [10] (left) and a fine lattice domain wall fermion calculation (right).

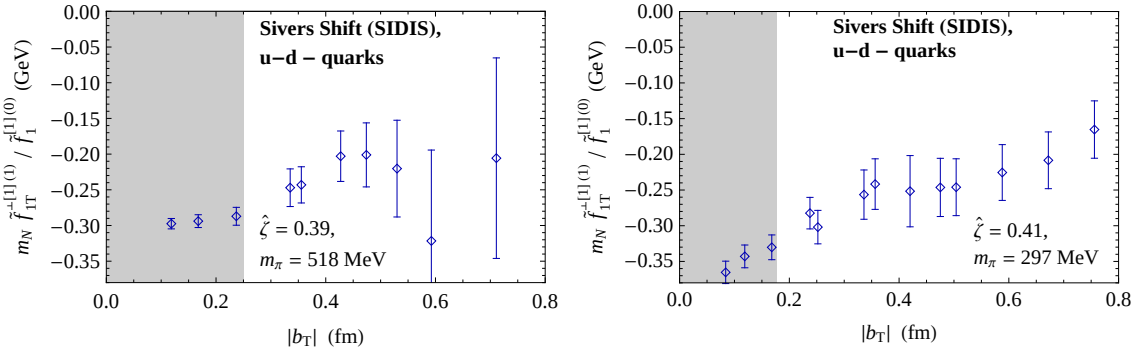

Figure 2: Generalized Sivers shift as a function of b_T in the $\eta \to \infty$ SIDIS limit, at a fixed $\hat{\zeta}$, in a coarse lattice mixed action calculation [10] (left) and a fine lattice domain wall fermion calculation (right).

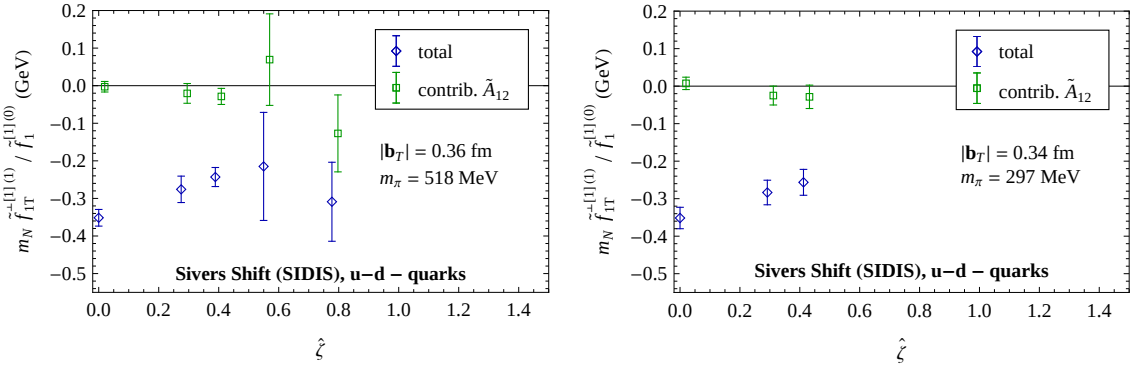

Figure 3: Generalized Sivers shift as a function of $\hat{\zeta}$ in the $\eta \to \infty$ SIDIS limit, at a fixed b_T, in a coarse lattice mixed action calculation [10] (left) and a fine lattice domain wall fermion calculation (right).

accuracy. This issue has been investigated at length in [11]. The present study focuses instead on another aspect, namely, whether TMD ratios of the type (2.4) and (2.5), which are designed to cancel soft factors and multiplicative renormalization constants, are indeed robust under changes of the discretization scheme and lattice cutoff. Figs. 1-6 present new data for the isovector[1] Sivers

[1] In the isovector, $u-d$ quark combination, diagrams with operator insertions in disconnected quark loops, which have not been evaluated, cancel.

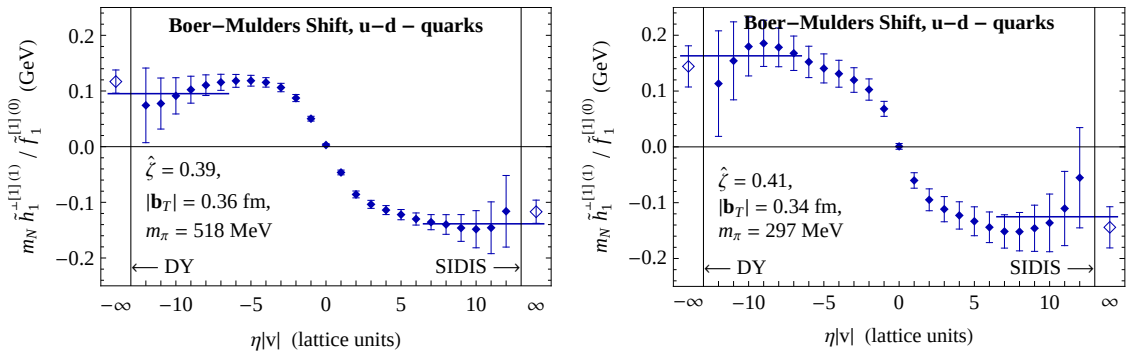

Figure 4: Dependence of the generalized Boer-Mulders shift on the staple extent at a fixed b_T and $\hat{\zeta}$, in a coarse lattice mixed action calculation [10] (left) and a fine lattice domain wall fermion calculation (right).

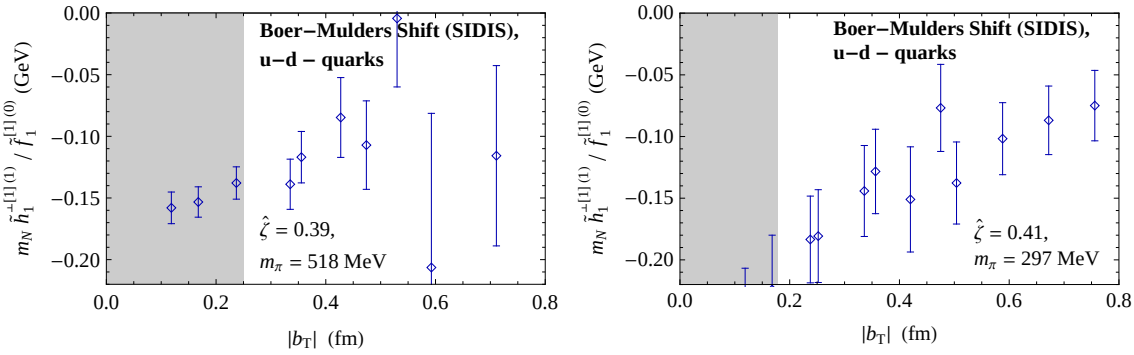

Figure 5: Generalized Boer-Mulders shift as a function of b_T in the $\eta \to \infty$ SIDIS limit, at a fixed $\hat{\zeta}$, in a coarse lattice mixed action calculation [10] (left) and a fine lattice domain wall fermion calculation (right).

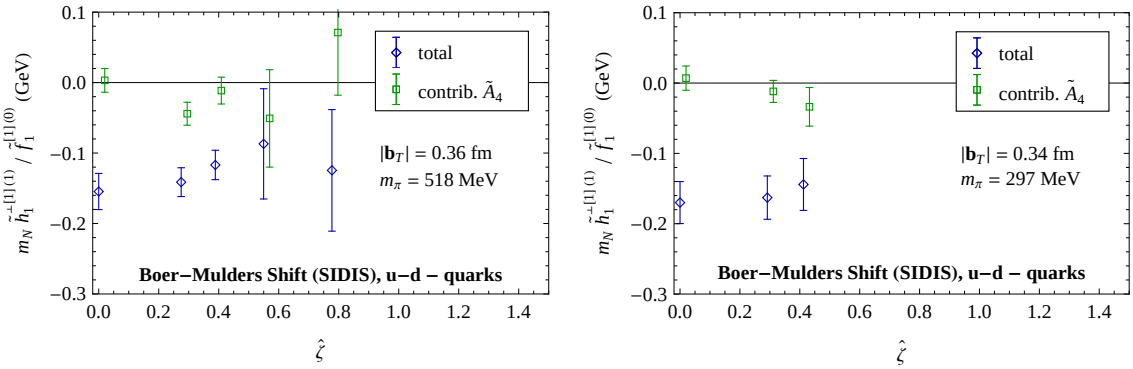

Figure 6: Generalized Boer-Mulders shift as a function of $\hat{\zeta}$ in the $\eta \to \infty$ SIDIS limit, at a fixed b_T, in a coarse lattice mixed action calculation [10] (left) and a fine lattice domain wall fermion calculation (right).

and Boer-Mulders shifts (2.4) and (2.5) in the nucleon, obtained using a RBC/UKQCD 2+1-flavor domain wall fermion ensemble with a lattice spacing of $a = 0.084\,\mathrm{fm}$, corresponding to a pion mass of $m_\pi = 297\,\mathrm{MeV}$. They are juxtaposed in Figs. 1-6 with corresponding data previously obtained [10] using domain wall valence quarks on a MILC 2+1-flavor gauge ensemble with a lattice spacing of $a = 0.12\,\mathrm{fm}$, corresponding to a pion mass $m_\pi = 518\,\mathrm{MeV}$. Note, thus, that the two ensembles differ significantly not only in discretization scheme and lattice cutoff, but also in

the pion mass. However, the previous mixed action study [10] revealed no significant dependence of the observables investigated here on the pion mass between $m_\pi = 518\,\mathrm{MeV}$ and $m_\pi = 369\,\mathrm{MeV}$, and therefore it is plausible to nevertheless view the comparison presented here primarily as a test for the presence of large discretization scheme and lattice cutoff effects.

Fig. 1 displays the dependence of the Sivers shift (2.4) on the staple extent for a given quark separation b_T and a given staple direction characterized by $\hat{\zeta}$. The T-odd behavior of this observable is evident, with $\eta \to \infty$ corresponding to the SIDIS limit, whereas $\eta \to -\infty$ yields the DY limit. The data level off to approach clearly identifiable plateaux as the staple length grows. The limiting SIDIS and DY values, represented by the open symbols, are extracted by imposing antisymmetry in η, allowing one to appropriately average the $\eta \to \pm\infty$ plateau values. Fig. 2 summarizes the results in the SIDIS limit for different b_T at a given $\hat{\zeta}$, where the shaded area below $|b_T| = 2a$ indicates the region where the results may be significantly affected by finite lattice cutoff effects. Finally, Fig. 3 summarizes the dependence of the Sivers shift on the Collins-Soper evolution parameter $\hat{\zeta}$, with $|b_T|$ kept fixed. Note that the total shift is represented by the blue data points; the green data points correspond to a certain partial contribution to the Sivers shift which vanishes at $\hat{\zeta} = 0$, but dominates the quantity at large $\hat{\zeta}$; comparison of the full Sivers shift with the partial contribution thus can give an indication of convergence towards the large $\hat{\zeta}$ limit. For further details, cf. [10]. The signal for the shifts quickly deteriorates as the nucleon momentum P, and thus $\hat{\zeta}$, is increased. No clear trend can be identified at the present level of accuracy as $\hat{\zeta}$ rises; connecting with perturbative evolution equations at large $\hat{\zeta}$ will represent a challenge for the present approach.

Clearly, the results for the Sivers shift obtained on the two ensembles are compatible, except for deviations at small separations $|b_T|$, where finite lattice cutoff effects are indeed expected. This is observed in spite of the considerable differences between the ensembles in terms of discretization scheme and lattice spacing (as well as pion mass, cf. comments further above). Another comparison focused on discretization and cutoff effects at essentially fixed pion mass will be possible in follow-up work employing a clover fermion ensemble at pion mass $m_\pi = 317\,\mathrm{MeV}$ and lattice spacing $a = 0.114\,\mathrm{fm}$, generated by K. Orginos and collaborators in the Jefferson Lab lattice group. Preliminary analysis of the corresponding data corroborates the findings presented here.

Figs. 4-6 present data for the Boer-Mulders shift (2.5) analogous to Figs. 1-3. The correspondence between the data obtained on the two analyzed ensembles persists. The relative uncertainties in the case of the Boer-Mulders shift are somewhat larger than in the case of the Sivers shift. One reason for this is that, if one separates the u- and d-quark contributions, the Sivers shifts in the two cases are of opposite sign (thus reinforcing each other in the $u-d$ difference), whereas the Boer-Mulders shifts are of the same sign, thus canceling each other to some extent.

4. Summary and outlook

Within a continuing exploration of TMD calculations using lattice QCD, the principal focus of the present work is an empirical study of the lattice discretization and cutoff dependence of TMD ratio observables of the type (2.4) and (2.5). TMDs are defined via hadron matrix elements of nonlocal operators containing staple-shaped gauge connections, cf. (2.1), such as to incorporate final/initial state interactions (for the SIDIS/DY processes, respectively). In addition to renormalization factors associated with the quark fields, the gauge connections call for the introduction of

more intricate soft factors in order to effect their regularization and renormalization. While these factors are expected to be multiplicative, no rigorous justification of this working assumption, in particular in the lattice formulation, is available. The data gathered in the present work permit an empirical assessment of whether TMD ratios of the type (2.4) and (2.5), defined such as to cancel multiplicative renormalization and soft factors, indeed behave in a stable manner under a significant change of the discretization scheme and cutoff. No substantive variation was detected in comparing the results for the TMD ratios obtained using the two ensembles under consideration. It should be noted that these two ensembles differ significantly not only in the discretization scheme and cutoff, but also in the pion mass; however, preliminary results from follow-up work using a clover fermion ensemble at a pion mass of $m_\pi = 317\,\mathrm{MeV}$ and lattice spacing $a = 0.114\,\mathrm{fm}$, which provides a more focused comparison with the domain wall fermion ensemble analyzed here, corroborate the findings of the present study.

Acknowledgements

Computations were performed using resources provided by the U.S. DOE through USQCD at Jefferson Lab, employing the Chroma software suite [12]. The MILC and RBC/UKQCD collaborations are gratefully acknowledged for providing the gauge ensembles analyzed in this work, as are K. Orginos (supported by DOE grant DE-FG02-04ER41302) and the Jefferson Lab lattice group (supported by DOE grant DE-AC05-06OR23177, under which Jefferson Science Associates, LLC, operates Jefferson Laboratory) for furnishing additional gauge configurations for follow-up work corroborating the findings of the present study. Support by the Heisenberg-Fellowship program of the DFG (P.H.), SFB/TRR-55 (A.S.), the RIKEN Foreign Postdoctoral Researcher Program (S.S.), and the U.S. DOE and the Office of Nuclear Physics through grants DE-FG02-96ER40965 (M.E.) and DE-SC0011090 (J.N.) is acknowledged. R.G., T.B. and B.Y. are supported by DOE grant DE-KA-1401020 and the LDRD program at LANL.

References

[1] D. Boer, M. Diehl, R. Milner, R. Venugopalan, W. Vogelsang, *et al.*, `arXiv:1108.1713`.

[2] M. Alekseev, *et al.*, COMPASS Collaboration, *Phys. Lett.* **B673** (2009) 127.

[3] A. Airapetian, *et al.*, HERMES Collaboration, *Phys. Rev. Lett.* **103** (2009) 152002.

[4] H. Avakian, *et al.*, CLAS Collaboration, *Phys. Rev. Lett.* **105** (2010) 262002.

[5] S. M. Aybat and T. C. Rogers, *Phys. Rev.* **D 83** (2011) 114042.

[6] J. C. Collins, *Foundations of Perturbative QCD* (Cambridge University Press, 2011).

[7] S. M. Aybat, J. C. Collins, J.-W. Qiu and T. C. Rogers, *Phys. Rev.* **D 85** (2012) 034043.

[8] J. C. Collins and T. C. Rogers, *Phys. Rev.* **D 87** (2013) 034018.

[9] M. Engelhardt, B. Musch, P. Hägler, J. W. Negele and A. Schäfer, *PoS* **LATTICE2012** (2012) 169.

[10] B. Musch, P. Hägler, M. Engelhardt, J. W. Negele and A. Schäfer, *Phys. Rev.* **D 85** (2012) 094510.

[11] M. Engelhardt, B. Musch, P. Hägler, J. W. Negele and A. Schäfer, *PoS* **LATTICE2013** (2014) 284.

[12] R. G. Edwards and B. Joó, SciDAC Collaboration, *Nucl. Phys. Proc. Suppl.* **140** (2005) 832.